Applied Energy 208 (2017) 1113–1127

Contents lists available at ScienceDirect

Applied Energy

journal homepage: www.elsevier.com/locate/apenergy

A computationally efficient pseudo-3D model for the numerical analysis of borehole heat exchangers

Giuseppe Brunetti[a,*], Hirotaka Saito[b], Takeshi Saito[c], Jiří Šimůnek[d]

[a] Department of Civil Engineering, University of Calabria, Rende, CS 87036, Italy
[b] Graduate School of Agriculture, Tokyo University of Agriculture and Technology, 3-5-8 Saiwaicho, Fuchu, Tokyo, Japan
[c] Graduate School of Science and Engineering, Saitama University, 255 Shimo-Okubo, Sakura-ku, Saitama, Japan
[d] Department of Environmental Sciences, University of California, Riverside, CA 92521, USA

HIGHLIGHTS

- A computationally efficient modeling framework is proposed.
- The modeling approach includes a widely used hydrological model.
- The model is validated against experimental data from two Thermal Response Tests.
- The validated model is used to perform a statistical sensitivity analysis.
- The influence of groundwater and lithologic heterogeneities is examined.

ARTICLE INFO

Keywords:
Geothermic
Heat transfer
Thermal response test
Modeling
Sensitivity analysis

ABSTRACT

Ground-Source Heat Pump (GSHP) systems represent one of the most efficient renewable energy technologies. Their efficiency is highly influenced by the thermal properties of the ground, which are often measured in-situ using the Thermal Response Tests (TRTs). While three-dimensional mechanistic models offer significant advantages over analytical solutions for the numerical interpretation of TRTs, their computational cost represents a limiting factor. Moreover, most of the existing models do not include a comprehensive description of hydrological processes, which have proven to strongly influence the behavior of GSHP. Thus, in this study, we propose a computationally efficient pseudo-3D model for the numerical analysis and interpretation of TRTs. The numerical approach combines a one-dimensional description of the heat transport in the buried tubes of the exchanger with a two-dimensional description of the heat transfer and water flow in the surrounding subsurface soil, thus reducing the dimensionality of the problem and the computational cost. The modeling framework includes the widely used hydrological model, HYDRUS, which can simulate the movement of water, heat, and multiple solutes in variably-saturated porous media. First, the proposed model is validated against experimental data collected at two different experimental sites in Japan, with satisfactory results. Then, it is combined with the Morris method to carry out a sensitivity analysis of thermal properties. Finally, the model is exploited to investigate the influence of groundwater and lithologic heterogeneities on the thermal behavior of the GSHP.

1. Introduction

Ground-source heat pump (GSHP) systems use ground or groundwater as a heating/cooling source by circulating a non-freezing solution inside of a vertically or horizontally installed closed-loop tube to transfer heat to/from the ground. Because GSHP systems are based on renewable energy and can achieve a much higher coefficient of performance (COP) than conventional air-source heat pump systems, the use of GSHP systems has been rapidly increasing worldwide. According to one of the most recent reviews by Lund and Boyd [1], the total installed capacity of ground-source heat utilization systems increased 46.2% worldwide from 2010 to 2014 and more than 600% in the past 20 years. Among different ground-source heat utilization systems, GSHP systems account for more than 70% of the installed capacity worldwide. The heat exchange capacity of the heat exchanger, which determines the performance of the GSHP systems, is mainly characterized by ground thermal properties, such as the thermal conductivity and the thermal capacity. As the optimum design and

* Corresponding author.
E-mail address: Giusep.bru@gmail.com (G. Brunetti).

http://dx.doi.org/10.1016/j.apenergy.2017.09.042
Received 24 April 2017; Received in revised form 31 July 2017; Accepted 10 September 2017
Available online 18 September 2017
0306-2619/

operation of GSHP systems depend on the heat exchange capacity, it is critical to know the ground thermal conductivity before the installation of the GSHP systems.

The apparent thermal conductivity of the ground can be obtained from one of many in-situ thermal conductivity tests. In many in-situ tests, the ground is considered to be homogeneous although it often displays clear heterogeneities, such as layering. It is common to neglect the effects of layering or heterogeneity when estimating the ground thermal conductivity. This assumption was recently investigated by Luo et al. [2], who analyzed two modeling approaches in which ground properties were considered to be either homogeneous or stratified. The comparison of fluid outlet temperatures between these two cases showed relatively minor differences, indicating that the assumption of a homogeneous ground introduces a relatively low bias and that the Thermal Response Tests or TRTs [3] are suitable to determine the effective thermal conductivity of the ground. TRTs are the in-situ tests most frequently used to estimate the apparent ground thermal conductivity and the borehole thermal resistance. In TRTs, a non-freezing solution or water is circulated inside of a closed-loop pipe installed vertically or horizontally in the subsurface while it is heated by a constant heat source at the inlet. The inlet and outlet fluid temperatures are then continuously recorded. These temperatures are later used to estimate thermal properties of the ground and the borehole. A number of in-situ mobile or immobile devices for TRT tests have been developed [4]. Furthermore, a number of data analysis methods, based on either simple analytical solutions or more complex numerical solutions, have been used to estimate thermal properties of the ground.

When a vertically installed heat-exchange well (which is in many cases 50–100 m long) is used, the closed-loop pipe is much longer in the vertical direction than its diameter, which is at most several tens of mm. For this reason, the data analysis typically uses an analytical solution that is either based on the line source function of Kelvin [5] or the cylindrical heat source theory [6]. The Kelvin's source function assumes a system in cylindrical coordinates with an infinitely long line heat source in the center. Under the assumptions that the heat flux from the heat source is constant regardless of time or depth, the medium has uniform thermal characteristics, and the heat transfer in the vertical direction can be neglected, the following analytical solution is obtained by solving the heat conduction equation that describes the change in the ground temperature ΔT at a given time t and distance r. It is also assumed that temperature at infinity is constant:

$$\Delta T = T(r,t) - T_i = -\frac{Q'}{4\pi\lambda} Ei(-s) = -\frac{Q'}{4\pi\lambda}\left(\gamma + \ln s - \sum_{k=1}^{\infty} \frac{(-1)^{k-1} s^k}{k \cdot k!}\right) \quad (1)$$

$$s = \frac{r^2 C}{4\lambda t} \quad (2)$$

where $Ei(-s)$ is the integral exponential function, Q' is the heat per unit length of the line heat source [M L T^{-3}], λ is the thermal conductivity [M L T^{-3}K^{-1}], C is the volumetric heat capacity [M L^{-1} T^{-2} K^{-1}], and γ is the Euler constant, which has a value of 0.5772 [5,6]. When t is large and s is sufficiently small ($s < 0.05$), Eq. (1) can be approximated using the thermal diffusivity parameter α ($=\lambda/C$) [L^2 T^{-1}] by the following equation:

$$\begin{aligned} \Delta T &= T(r,t) - T_i = -\frac{Q'}{4\pi\lambda}\left(\ln\frac{r^2}{4\alpha t} + 0.5772\right) \\ &= \frac{Q'}{4\pi\lambda}\ln(t) - \frac{Q'}{4\pi\lambda}\left(\ln\frac{r^2}{4\alpha} + 0.5772\right) \\ &= m\ln(t) + b \\ m &= \frac{Q'}{4\pi\lambda}, \quad b = -\frac{Q'}{4\pi\lambda}\left(\ln\frac{r^2}{4\alpha} + 0.5772\right) \end{aligned} \quad (3)$$

In practice, the average fluid temperature between an inlet and an outlet of the U-tube during TRT is taken as $T(0, t)$ in Eq. (3) to estimate λ. The most straightforward approach is to plot $T(0, t)$ as a function of the natural logarithm of time. The thermal conductivity λ can then be estimated from the slope m of the plot. This estimate depends largely on the selection of the temporal data section. By selecting the time period, during which there is an obvious linear relationship, early time data are discarded from the analysis. Also, since the volumetric heat capacity C (or the specific heat c) that characterizes the heat storage in a substance is not estimated [7], C must be obtained by another method.

In addition to ignoring the effects of heterogeneity of the geological system and its three-dimensionality, the analytical solution based on the line source solution of Kelvin cannot easily account for several practical issues, such as variations in ambient temperatures during the test [8] or variations or instability in the heating source at the inlet [9]. It should be emphasized that the heat transfer is not solely due to conduction, but also a result of convection due to regional groundwater flow. In a region where groundwater flow is relatively fast, one can expect a higher heat exchange rate. Multiple studies have investigated the effect of groundwater flow on borehole heat exchangers (BHE). For example, Liuzzo-Scorpo et al. [10] demonstrated that even very low groundwater flow rates can significantly reduce the Influence Length of the exchanger. In another study, Wang et al. [11] conducted a thermal performance experiment of a BHE under groundwater flow in China and showed that the presence of groundwater flow enhanced the thermal performance of the borehole heat exchanger and influenced the temperature profile in the aquifer. Although recent studies have proposed complex analytical solutions [12], such effects are not taken into account in most of them considering the high nonlinearity and mutual interactions of hydrological and thermal processes involved. These interactions were properly emphasized in a recent study of Liuzzo-Scorpo et al. [13], where the authors proposed a fast graphical method to estimate the hydraulic conductivity of the aquifer using the TRT analysis.

It is thus necessary to develop more reliable and more robust approaches that can account for the above-discussed factors affecting ground heat exchange so that ground thermal properties may be more accurately estimated. For example, numerical solutions of the equations governing the phenomena related to ground heat exchange processes have been coupled with parameter estimation procedures to estimate thermal properties from TRT data [14]. Numerical approaches provide much more flexibility in accounting not only for more physical processes, detailed geometry, and different materials, but also for various initial, boundary, and operational conditions that are usually oversimplified when analytical solutions are used. Numerical models, therefore, allow more detailed representations of the system and phenomena related to TRT. More importantly, by using numerical solutions, we do not need to omit early time data of TRT, which are usually discarded, when estimating ground thermal properties using analytical approaches [15]. By being able to use early data, which reflect thermal properties of the tube and the grout, it is possible to estimate thermal properties of different materials composing the system. There have been numerous studies that have used numerical models. These studies usually employed the Finite Difference (FD), Finite Elements (FE), or Finite Volume (FV) methods. Florides et al. [16] applied a model that combined three-dimensional (3D) conduction with one-dimensional (1D) mass flow and 1D convective heat transfer within the carrier fluid. The resulting 3D model was implemented in the FlexPDE® environment and used to investigate the thermal performance of single and double U-tube borehole heat exchangers in multiple-layer substrates. However, the effect of groundwater was neglected by Florides et al. [16]. A similar approach was used by Ozudogru et al.[17], who coupled the commercial software COMSOL® for the description of the heat transfer in the borehole with a 1D description of heat and water transport in the pipe. In another study, Han et al. [18] developed a 3D coupled Finite Element Model, which was then utilized to simulate steady-state and transient behaviors of a geothermal heat exchanger. Han et al. [18] validated the model and then used it to investigate the influence of several factors on the borehole behavior by carrying out a sensitivity analysis. However, one of the main disadvantages of 3D mechanistic models is their computational cost, which limits their use in

conjunction with parameter estimation algorithms. Thus, more research is needed to develop accurate and computationally efficient models.

When the numerical approach is adopted to analyze the TRT data, special attention needs to be paid to a dramatically different dimensionality of the tube and the ground. While the thickness of the tube is on the order of several millimeters, the tube length and the geological system are usually on the order of a hundred or even several hundred meters. Signorelli et al. [19] used the finite-element-based numerical code FRACTure [20] to evaluate the effect of factors not considered by analytical solutions since his code allowed one to use a combination of lower and higher dimension elements. In their analysis, a one-dimensional model was used for heat transport in tubes, while a three-dimensional model was used to simulate heat transfer in the surrounding ground. Bozzoli et al. [21] took a similar modeling approach where both one- and three-dimensional equations were solved for different domains to inversely estimate thermal properties of the soil and the grout. In their analysis, the heat transfer between the fluid inside the tube and the solid phase (e.g., tube or grout) was modeled using the Robin boundary condition with the heat transfer coefficient, which is a function of fluid parameters. Instead of using the Robin boundary condition, Christodoulides et al. [22] used a source/sink term in the governing equation to account for the heat transfer between the fluid and the tube, assuming the heat transfer within the tube body was instantaneous because the thickness of the tube was extremely thin. An interesting modeling approach was proposed by Kim et al. [23], who applied a Model Order Reduction (MOR) technique to develop a computationally efficient model for the numerical analysis of a vertical borehole heat exchanger. Kim et al. [23] combined a vertical slice model with a Finite Element discretization of horizontal cross sections and validated it against analytical solutions. The authors reported a computational time reduction of 95% compared to a fully 3D model. However, the proposed model lacked a proper description of hydrological processes in the vadose zone, which proved to significantly affect the thermal performance of the borehole heat exchanger.

In this view, another factor that is usually excluded from the analysis is the effect of the mass and energy transport in the unsaturated zone, which usually surrounds a significant portion of the vertically installed well. In the case of horizontally installed U-tubes, surrounding soils are often unsaturated. The computational cost of evaluating flow and transport processes in the unsaturated zone is significantly higher than in the saturated zone. This may become an issue when numerical approaches are used, especially for three-dimensional models. Developing a numerically efficient method that can account for detailed saturated-unsaturated processes is therefore essential in promoting a numerical data analysis of borehole heat exchangers. Since GSHP are strongly influenced by hydrological processes occurring in the vadose zone, it is necessary to bridge the gap and develop models that are able to describe the thermal and hydrological behavior of the entire ground-borehole system.

Thus, the first objective of this study was to develop a computationally efficient pseudo-3D model for the numerical analysis and interpretation of TRTs. The numerical approach combines a one-dimensional description of the heat transport in the buried tubes of the exchanger with a two-dimensional description of the heat transfer in the surrounding subsurface soil, therefore reducing the dimensionality of the problem and the computational cost. Furthermore, the modeling framework includes the widely used hydrological model, HYDRUS [24], which can simulate the movement of water, heat, and multiple solutes in variably-saturated porous media. The combination of a reduced-order numerical approach with a hydrological model guarantees a high modeling flexibility and represents a new contribution to this field. The second objective of this study is to validate the newly developed model against experimental data collected at two different experimental sites in Japan and to use the validated model to carry out a sensitivity analysis, based on the Morris method [25], that would investigate the influence of different materials on the TRT response. Finally, the third objective is to demonstrate the capability of the model to handle various hydrological processes in the vadose zone by investigating the influence of groundwater flow and aquifer thickness on the borehole heat exchanger. A further scenario has been used to demonstrate the ability of the proposed modeling framework to simulate the effect of layered soil profiles on the heat transfer process.

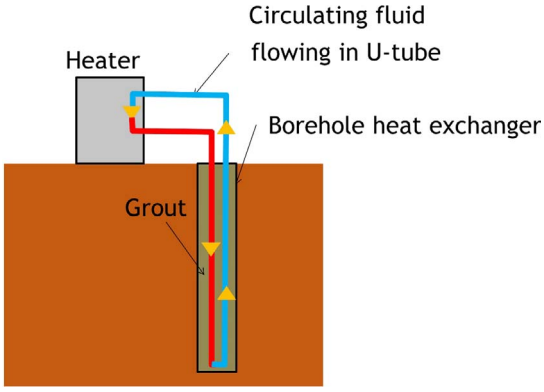

Fig. 1. A schematic of the experimental setup used to perform the thermal response test.

2. Materials and methods

2.1. Site description

The Thermal Response Tests (TRT) were performed at the campuses of Tokyo University of Agriculture and Technology (TUAT) (Fuchu city, Tokyo; 35°40′59″N, 139°28′58″E) and Saitama University (SU) (Saitama city, Saitama; 35°51′44″N, 139°36′34″E) in Japan. A schematic of the experimental setup is shown in Fig. 1. Two 50-m long vertical boreholes with an inner diameter of 180 mm were drilled in 2011 at TUAT to be used as borehole heat exchangers for a ground-source heat pump system installed for a 25 m^2 constant temperature room [26]. Without finishing with casing, two U-shaped 3-mm thick 20-mm diameter pipes made of high-density polyethylene (HDPE) were inserted into the borehole along with space-filling grout, which consisted mainly of silicate sand. Two U-shaped pipes were inserted together into the borehole since the bottom of both tubes were connected. The groundwater table at TUAT was 10–12 m below the ground surface. At SU, a 50-m long vertical borehole with an inner diameter of 180 mm was also drilled in 2011 to be used for a long-term heating and cooling experiment [27]. Similar to TUAT, two U-shaped 3-mm thick HDPE pipes were installed in the borehole. Silica sand was used as a space-filling grout material. The groundwater table at SU was 1–4 m below the ground surface.

Fig. 2 shows the distribution of particle sizes, water contents, and bulk densities measured at boring core samples collected at both BHE [28]. The particles greater than 2 mm (i.e., gravel) were excluded from the particle size distribution analysis. While the elevation of the TUAT site, which is located at the Tachikawa terrace, is about 60 m above the mean sea level (MSL), that of the SU site, which is in the Arakawa Lowland near the Tokyo metropolis, is about 10 m above MSL. At the TUAT site, there are three layers of gravel located at depths of 5–11 m, 32–34 m, and 43–45 m, where particle size distribution data were not available (or where water content values were very small due to low water retention of gravel). The average gravel content in each layer was 0.785 kg kg^{-1}, 0.848 kg kg^{-1}, and 0.808 kg kg^{-1}, respectively. At the SU site, a gravel layer was observed only around the depth of 40 m. On top of the gravel layer, silt layers and sand layers were deposited alternately.

During TRT, a non-freezing solution of 20% propylene glycol was heated to keep the temperature difference between the inlet and outlet at 4.5 °C with a constant power of 2.5 kW for 48 h while the fluid was

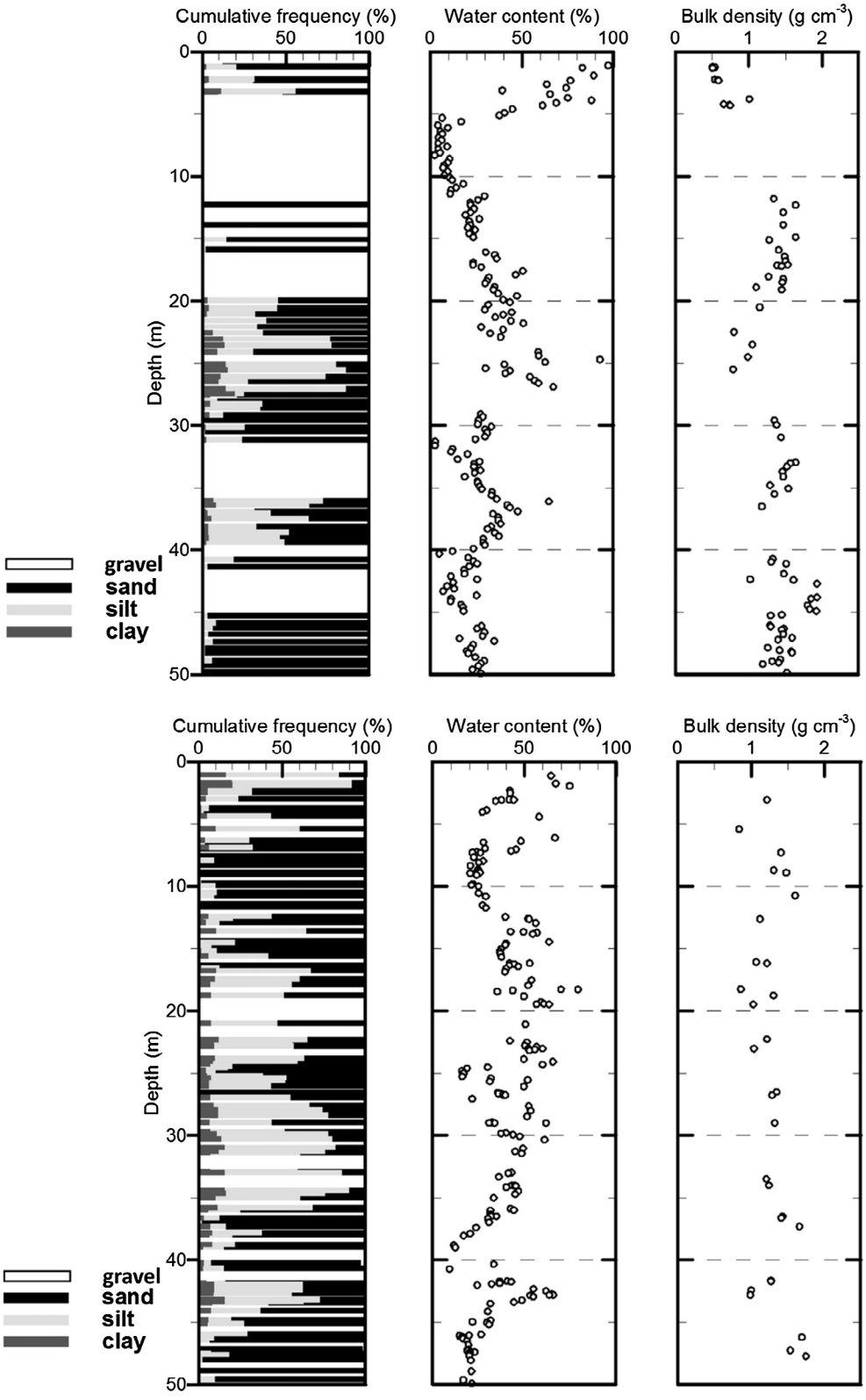

Fig. 2. Particle size distributions, water contents, and dry bulk densities from core samples collected at TUAT (the upper plot) and SU (the lower plot), respectively.

circulated at a constant rate of 9.0 L min^{-1} in one of the U-tubes in one HEB at TUAT. The temperatures of inlet and outlet fluid were continuously measured using a platinum temperature sensor whose measurement accuracy was less than 0.1 °C. As a result, the average heat exchange rate at the TUAT site was estimated to be 28.2 W m^{-1}. At SU, tap water was circulated in both U-tubes for 48 h with a constant heating power of 2.5 kW at a constant flow rate of 13.5 L min^{-1}. As a result, the average heat exchange rate at SU was estimated to be 56.4 W m^{-1}. The inlet–outlet temperature difference was kept at 3 °C. In the following analysis of the SU data, instead of using the double U-tubes, we assumed a single U-shape tube and used an effective radius of 3.7 mm which resulted in the surface area equal to the original double U-shape tubes.

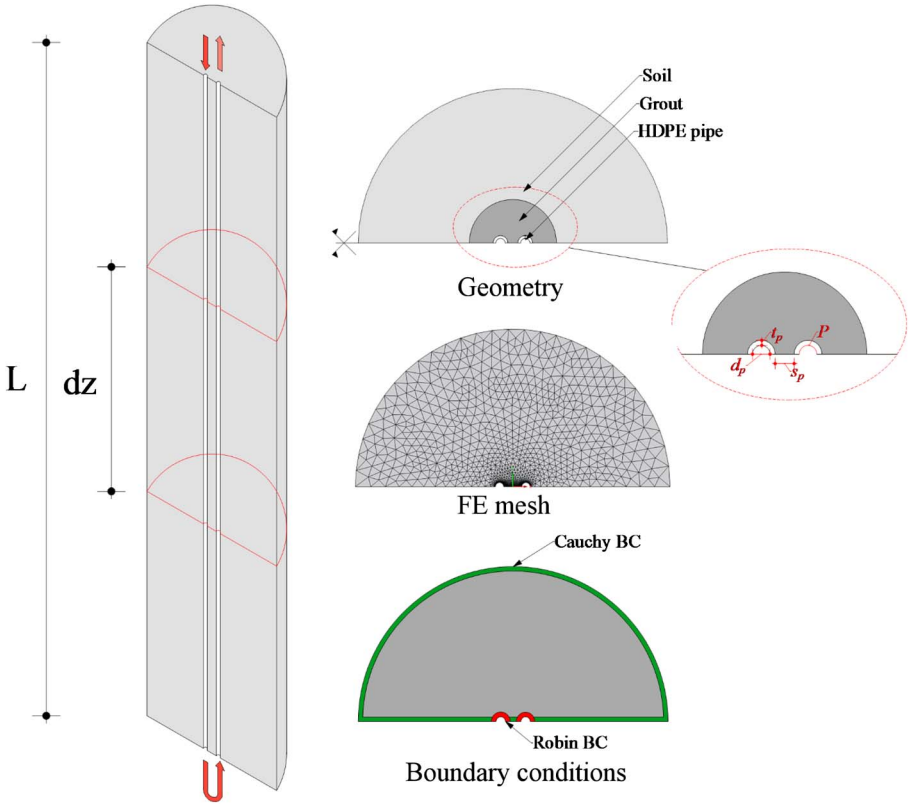

Fig. 3. A schematic of the modeled transport domain consisting of the subsurface soil and two branches of the heat exchanger.

2.2. Modeling theory

2.2.1. Modeling approach

A computationally efficient pseudo 3D-model for the numerical analysis of heat transfer in borehole heat exchangers has been developed in this study. The proposed approach combines a one-dimensional description of the heat transport in the buried tubes of the exchanger with a two-dimensional description of the heat transfer in the surrounding subsurface soil. The main assumption is that the heat transfer in the soil domain occurs only in the horizontal plane. Similar approaches have been proposed by Yavuzturk et al. [29] and Austin et al. [30]. However, the main novelty of the present study is the use of the well-established hydrological model, HYDRUS, in the modeling framework.

The vertical three-dimensional soil profile is discretized in N two-dimensional horizontal cross-sections. Each cross-section contains two nodes of the one-dimensional fluid domain (Fig. 3), which represent the two branches of the tube. The heat transfer between the two domains, i.e., between two-dimensional cross sections and a one-dimensional tube, is represented by a Robin boundary condition. The reduced dimensionality of the proposed approach guarantees a significant computational gain compared to a fully three-dimensional model while maintaining a comparable accuracy. However, it must be emphasized that the proposed approach neglects the effects of natural convection (and other vertical, parallel with the borehole, heat fluxes) on the borehole that may occur under saturated conditions and that may enhance the heat transfer and reduce the thermal resistance of the borehole. The magnitude of the natural convection depends on the temperature difference between the fluid in the U-tube and the surrounding ground and it is thus directly related to the heat injection rate. Gustafsson and Gehlin [31] reported a decrease of more than 10% in the borehole thermal resistance when the heat injection rate increased from 40 W/m to 80 W/m. As pointed out by Spitler et al. [32], this process is rather significant for groundwater-filled borehole heat exchangers in which groundwater fills the annular space between the U-tube and the borehole wall, while it is less pronounced for cement-grouted borehole heat exchangers, as reported by Choi and Ooka [33]. Choi and Ooka [33] also emphasized how the effect of the natural convection in the borehole was mainly dominated by the hydrothermal properties of the surrounding soil, rather than the filling material. In particular, the permeability of the soil is directly related to the magnitude of the buoyancy flow [34].

The modeling approach proposed in this study should be used carefully in scenarios when the borehole is filled with groundwater and when relatively high heat injection rates are used as these could lead to biased results. Under such circumstances, more complex 3D models should be adopted.

2.2.2. One-dimensional heat transport in the vertical domain

The heat transport in both tubes of the heat exchanger is assumed to be one-dimensional and purely advective [14]:

$$\rho_f c_f \frac{\partial T_f}{\partial t} = \rho_f c_f u \frac{\partial T_f}{\partial z} \tag{4}$$

where ρ_f is the density of the fluid [M L^{-3}], c_f is the specific heat capacity of the fluid [L^2 T^{-2} K^{-1}], T_f is the temperature of the fluid [K], u is the fluid velocity [L T^{-1}] (positive for the descending tube and negative for the ascending tube), and z is the vertical coordinate [L] assumed positive downward. The convective heat transfer between the tube and the fluid was described by a source term added to Eq. (4), which becomes:

$$\rho_f c_f \frac{\partial T_f}{\partial t} = \rho_f c_f u \frac{\partial T_f}{\partial z} - \frac{h}{A_f} \int_P [T_f(z,t) - T_p(p,z,t)]\, dp \tag{5}$$

where h is the heat transfer coefficient [M T^{-3} K^{-1}], P is the pipe inner perimeter [L], T_p is the temperature on the inner surface of the pipe [K], and A_f is the area of the tube [L^2]. The integral in the last term of (5) averages the temperature between the fluid and the HDPE pipe along its inner perimeter. Eq. (5) can be written also as:

$$\rho_f c_f \frac{\partial T_f}{\partial t} = \rho_f c_f u \frac{\partial T_f}{\partial z} + \frac{h}{A_f}\int_P T_p(p,z,t)dp - \frac{4h}{d_p}T_f(z,t) \quad (6)$$

where d_p is the inner diameter of the pipe [L] (Fig. 2).

The convective heat transfer coefficient can be estimated using the relation:

$$h = \frac{\lambda_f}{d_p}Nu \quad (7)$$

where λ_f is the thermal conductivity of the fluid [M L T^{-3} K^{-1}], and Nu is the Nusselt number [–], which is expressed using the Dittus-Boelter correlation as:

$$Nu = 0.023Re^{0.8}Pr^n \quad (8)$$

where Re is the Reynolds number [–], Pr is the Prandtl number [–], and n is a coefficient assumed to be 0.33 for cooling (the wall hotter than fluid) and 0.4 for heating (the wall colder than fluid).

Eq. (6) has been solved using the Finite Volume Method (FVM). A second-order accurate QUICK (Quadratic Upstream Interpolation for Convective Kinematics) scheme [35] has been adopted due to its capability to reduce the artificial numerical dispersion and achieve a good accuracy of the solution. A semi-implicit time stepping scheme has been used. The first (i.e., advective component) and second terms on the right-hand side of Eq. (6) have been solved explicitly in time, while the third term has been solved implicitly. The linearization of the second term, which is a function of the temperature of the tube wall, allows for a significant reduction of the computational cost. An implicit treatment of this term would have required running a two-dimensional model for the soil domain several times at each time step, significantly increasing the simulation time.

The problem definition was completed by the specification of the initial and boundary conditions. The condition of a constant power supplied to the fluid has been implemented using a periodic Dirichlet condition for the descending tube:

$$T_f^{descending}(0,t) = T_f^{ascending}(0,t) + \Delta T \quad (9)$$

where ΔT is a constant temperature increment [K]. The U-tube connection was modeled by imposing the same temperature on the two legs of the tube at z = L, which was numerically accomplished by using a Dirichlet boundary condition for the ascending pipe. The one-dimensional heat transport in the vertical domain has been solved numerically in the Python programming language.

2.2.3. Two-dimensional heat transport in the horizontal domain

The HYDRUS (2D/3D) software [24] has been used to simulate the heat transport in the horizontal domains. The software contains a two-dimensional finite element model HYDRUS-2D for simulating the movement of water, heat, and multiple solutes in variably-saturated porous media. Neglecting the effects of water vapor diffusion, two-dimensional heat transport can be described as:

$$C(\theta)\frac{\partial T_s}{\partial t} = \frac{\partial}{\partial x_i}\left(\lambda_{ij}(\theta)\frac{\partial T_s}{\partial x_j}\right) - C_f q_i \frac{\partial T_s}{\partial x_i} \quad (10)$$

where $C(\theta)$ and C_f are the volumetric heat capacities of the solid and liquid phases, respectively [M L^{-1} T^{-2} K^{-1}], θ is the volumetric water content [–], $\lambda_{ij}(\theta)$ is the apparent thermal conductivity of the soil [M L T^{-3} K^{-1}], and q_i represents the water flux in the porous media [L T^{-1}]. The first term on the right-hand side of Eq. (10) represents the heat transfer by conduction in the soil, while the second term accounts for heat being transported by flowing water. The apparent thermal conductivity $\lambda_{ij}(\theta)$ combines the thermal conductivity $\lambda_0(\theta)$ of the porous medium in the absence of flow and the macrodispersivity, which is assumed to be a linear function of the velocity. It can be expressed as:

$$\lambda_{ij}(\theta) = \lambda_T C_w |q| \delta_{ij} + (\lambda_T - \lambda_L) C_w \frac{q_j q_i}{|q|} + \lambda_0(\theta)\delta_{ij} \quad (11)$$

where δ_{ij} is the Kronecker delta function, and λ_L and λ_T are the longitudinal and transverse thermal dispersivities [L]. $\lambda_0(\theta)$ is described with the equation [36]:

$$\lambda_0(\theta) = b_1 + b_2\theta + b_3\theta^{0.5} \quad (12)$$

where b_1, b_2, and b_3 are empirical parameters [M L T^{-3} K^{-1}].

The convective heat transfer between the fluid and the solid domain has been described using a Robin boundary condition (Eq. (13)):

$$\lambda_{ij}\frac{\partial T_s}{\partial x_j}n_i = h\cdot[T_f - T_{p_i}] \quad (13)$$

where T_{pi} is the temperature on the inner surface of the tube [K].

Since the Robin BC is not included in the standard version of HYDRUS, an *ad hoc* version has been developed. Once the fluid temperature and the convective heat transfer coefficient are specified, HYDRUS automatically updates the value of the heat flux at the boundary. HYDRUS-2D uses an implicit adaptive time stepping to solve Eq. (10), thus minimizing the computational cost and guaranteeing the accuracy of the solution.

A Cauchy-type boundary condition was specified on the remaining boundaries of the domain (green[1] line in Fig. 2). The Cauchy BC prescribes the heat flux along the boundary, and can be expressed as:

$$-\lambda_{ij}\frac{\partial T_s}{\partial x_j}n_i + TC_f q_i n_i = T_0 C_f q_i n_i \quad (14)$$

in which T_0 is the temperature of the incoming fluid. When the boundary is impermeable or when water flow is directed out of the region, Eq. (14) reduces to a Neumann type BC of the form:

$$\lambda_{ij}\frac{\partial T_s}{\partial x_j}n_i = 0 \quad (15)$$

2.2.4. Models coupling strategy

The one-dimensional vertical domain and the two-dimensional cross-sectional domains have been coupled using a Python script, which acted as a "glue" between the two models. The script simultaneously solves the 1D advective heat transport in the tube, interacts with HYDRUS-2D, and exchanges data between the two models. As mentioned previously, a horizontal HYDRUS-2D cross section was located at each node of the 1D fluid domain. The coupling strategy is summarized below:

1. A common time step is set for both models;
2. The simulation begins with the numerical discretization of the vertical domain for both legs of the U-tube. Python reads the temperatures on the border of the cross-sectional domains and solves Eq. (6), updating the values of the fluid temperature in different nodes;
3. A *for* loop is used to iterate through different horizontal cross-sections. At each iteration, the initial condition is first updated and the calculated fluid temperatures are passed to the HYDRUS solver for the computation of the Robin boundary condition. HYDRUS-2D is then executed and the resulting calculated solid temperatures are stored in a 2D matrix for the next time step. This matrix contains temperature distributions for all horizontal cross sections and is updated at each time step.

An important feature of this approach is that each horizontal cross-section can have its own hydraulic and thermal properties reflecting different geological layers and their saturations, which guarantees a significant modeling flexibility.

[1] For interpretation of color in Fig. 2, the reader is referred to the web version of this article.

2.3. Model validation

2.3.1. Objective function

To assess its accuracy, the model was validated against experimental data collected at two experimental facilities described above. In particular, the measured and simulated outlet temperatures were compared. The use of the fluid outlet temperature as a reference data for validating the model is widespread in conventional TRTs. However, it must be emphasized that limited information content of the outlet temperatures does not allow for a precise estimation of thermal properties of different soil layers. Beier et al. [37] investigated the usefulness of different experimental data sets for the TRT analysis and model validation. Beier et al. [37] also considered, in addition to usual measurements of outflow temperatures, temperatures measured on the borehole wall and in the surrounding soil. The analysis revealed that both data sets can be used to better constrain the parameter estimation and provide independent validation measurements. For example, thermal probe data can provide an independent measurement of the soil thermal conductivity. This information can be used to validate optimized parameters or as prior information in the Bayesian inference framework.

In the present study, the Root Mean Square Error (*RMSE*) was used to quantify the overall quality of the fit:

$$RMSE = \sqrt{\frac{\sum_{i=1}^{n} (T_{obs,i} - T_{\mathrm{mod},i})^2}{n}} \tag{16}$$

where $T_{obs,i}$ is the ith measured temperature [K], $T_{mod,i}$ is the ith modeled temperature [K], and n is the number of observations. The *RMSE* is a common choice in borehole model validation and the TRT analysis [38].

2.3.2. Numerical domain and boundary conditions

The thermal properties were taken from a previous study of Saito et al. [39], which was carried out at the same experimental facilities. Only the thermal properties of the grout for the TUAT experimental site were manually adjusted to increase the overall accuracy of the fit. The thermal properties that were used for model validation in both case studies are listed in Table 2. Since FVM schemes can be affected by false numerical diffusion when the velocity of the simulated process is relatively high and when the mesh size is large, a preliminary sensitivity analysis has been carried out to investigate the influence of the vertical discretization on the numerical solution. Usually, a combination of higher order schemes and fine mesh sizes is needed to reduce the false numerical diffusion. However, the use of a very fine vertical discretization would have increased the computational cost of the analysis. Thus, the main aim of the preliminary mesh sensitivity analysis was to establish a balanced vertical discretization, guaranteeing both a high accuracy and a reasonable computational cost of the numerical solution.

The domain was discretized into two-dimensional triangular elements using the MESHGEN tool of HYDRUS-2D. The mesh was refined near the pipes to accommodate the significant temperature gradients generated by the convective heat transfer, therefore increasing the overall accuracy of the solution. The generated FE mesh had 1114 and 1234 nodes, and 2117 and 2346 two-dimensional elements for the TUAT and SU experimental site, respectively. The Robin BC was used to simulate the heat transfer between the carrier fluid and the pipes, while a Cauchy BC was used for the remaining boundaries. The initial temperatures and input parameters are summarized in Table 1.

Table 2
Thermal properties (thermal conductivity λ and thermal capacity *C*) of various materials (HDPE is a pipe material, high-density polyethylene) used in the model validation.

Material	Parameter	TUAT	SU
HDPE	Thermal conductivity λ_p[‡] (W/m^2 K)	0.51	0.51
	Volumetric heat capacity C_p (MJ/m^3 K)	1.71	1.71
Grout	Thermal conductivity λ_g (W/m^2 K)	1.70	2.80
	Volumetric heat capacity C_g (MJ/m^{3}K)	1.20	3.10
Soil	Thermal conductivity λ_s (W/m^2 K)	2.28	1.70
	Volumetric heat capacity C_s (MJ/m^3 K)	3.10	3.10

[‡] Subscripts *p*, *g*, and *s* refer to HDPE, grout, and soil, respectively.

Table 1
Geometric characteristics, thermal properties of different materials, and input parameters used in the numerical simulation.

	TUAT	SU
Internal diameter of the U-tube, d_p (m)	0.020	0.037
U-tube thickness, t_p (m)	0.003	0.003
U-tube length, L (m)	50	50
Fluid velocity, u_f (m s^{-1})	0.15	0.21
Heat transfer coefficient, h (W m^{-2} K^{-1})	834.7	1038.1
Initial temperature, T_0 (K)	290.15	289.35
Inlet-outlet temperature difference, ΔT (K)	4.5	3
Fluid density, ρ_f (kg m^{-3})	1000	1000
Fluid specific heat, c_f (J kg^{-1} K^{-1})	4182	4182
HDPE density, ρ_p (kg m^{-3})	950	950
HDPE specific heat, c_p (J kg^{-1} K^{-1})	1800	1800
HDPE thermal conductivity, λ_p (W m^{-1} K^{-1})	0.51	0.51
Diameter of the heat exchange well, d_w (m)	0.178	0.178

Considering that only the inlet and outlet fluid temperatures were measured, the soil profile was assumed to be homogeneous, thus neglecting the effects of different soil textures. Moreover, the heat transfer in the porous medium was assumed to be independent of the volumetric water content, i.e., the contribution of the terms with the parameters b_2 and b_3 to the thermal conductivity (see Eq. (12)) was neglected. The inclusion of these parameters in the inverse analysis would increase the dimensionality of the inverse problem and pose a parameter identification problem, considering that only one type of measured data (i.e., outlet temperature) was available for the analysis. The overall analysis was conducted with a laptop equipped with a CPU Intel® Core i7-4700 MQ 2.40 GHz processor and 8 GB of RAM.

2.4. Sensitivity analysis

2.4.1. Morris method

The main aim of developing an accurate and reliable model is to potentially exploit it to analyze different components of the simulated process. A classic example is to use the model to investigate the effects of different parameters on some variables of interest, namely a sensitivity analysis. For example, Florides et al. [40] used a previously validated three-dimensional finite element model to examine the influence of the ground properties on the thermal behavior of a borehole heat exchanger. In particular, authors highlighted how the soil thermal conductivity plays a major role toward dissipating the heat into the ground as well as when this sensitivity starts increasing with time. In another study, Wagner et al. [41] used a three-dimensional finite element model to investigate the effect of a shank spacing, a non-uniform initial thermal distribution, and the thermal dispersivity on a thermal response test. However, the main limitation of such types of sensitivity analyses is their lack of a rigorous statistical base.

The Morris method [25] belongs to the class of *Screening methods* (SM). SMs aim to provide qualitative sensitivity measures for different factors using a relatively small number of model evaluations. In general, the Morris method is a one-factor-at-a-time (OAT) local method, since it computes the *elementary effect* by changing only one factor at a time. However, it can be viewed as a Global method, since it averages several elementary effects computed at different points in the parameter space, providing a qualitative measure of the importance and interactions of different factors.

In this study, the modified version of the Morris method proposed

by Campolongo et al. [42] has been used to investigate the influence of thermal properties of ground, grout, and pipe on the TRT response. σ and μ^* are the two sensitivity measures calculated in the Morris method. While the former summarizes the interaction effect, the latter reflects the overall importance of a particular parameter. For a detailed description of the method, refer to Morris [25] and Campolongo et al. [42]. To interpret the results by simultaneously taking into account both sensitivity measures, Morris suggested their graphical representation in the (μ^*–σ) plane.

The sensitivity analysis has been performed for two different simulation durations of 10,800 and 30,000 s to examine the dynamics of the sensitivity measures. Although, for the sake of simplicity, the analysis has been applied only to the TUAT experimental site, its results can be generalized. The *RMSE* has been used as the objective function in the sensitivity analysis. Considering the computational cost of the model and the intent of the present analysis, which was targeted to a qualitative evaluation of the parameters influence, the sample size was set to 5, with a total of 35 numerical simulations for each scenario.

2.4.2. Groundwater effects

As reported by Signorelli et al. [19], groundwater flow can significantly affect borehole heat exchangers when groundwater fluxes are equal to or above 10^{-1} m/s, which can occur in permeable aquifers or regions with high hydraulic gradients. In particular, groundwater can enhance the performance of the system by dissipating heat around boreholes faster than unsaturated soil. Moreover, groundwater can introduce significant nonlinearities in the measured temperatures which cannot be interpreted accurately with a simplified model based on an infinite line source. It must be emphasized that while previous modeling studies have already investigated the effect of groundwater [19,43,44], none of these studies could fully exploit the features of a complex hydrological model, such as HYDRUS, which can give a comprehensive description of a variety of subsurface physical processes.

The proposed modeling framework has been used to investigate the influence of groundwater on the borehole heat exchanger. In particular, the effects of the aquifer thickness and groundwater flow have been examined. A 50-m long U-tube borehole heat exchanger, similar to the one used at the TUAT experimental site, has been simulated. The soil profile was assumed to be homogeneous and composed of sand. The thermal properties of a typical sandy soil are reported in Table 3.

Three different aquifer thicknesses were simulated: 10, 20, and 30 m. The Python code automatically overwrites the initial pressure head at each time step depending on the vertical coordinate of the Finite Volume calculated. A pressure head of -1 m, which corresponds to $\theta \approx 0.05$ for sandy soils, is imposed above the water table. A positive pressure head (full saturation) is set below the water table.

Similarly, the effect of groundwater flow in a 30-m deep unconfined aquifer on the TRT response has been simulated. Three different water flow values were considered: 0.0, $2.5 \cdot 10^{-6}$, and $5 \cdot 10^{-6}$ m/s. Water flow was simulated in HYDRUS-2D using the constant flux BC, with a water temperature of 290.15 K. The input parameters (i.e., the U-tube thickness, fluid velocity, the inlet-outlet temperature difference, etc.) and other thermal properties (i.e., HDPE, grout) were the same as those used for the TUAT model validation. A schematic of the analyzed scenario is reported in Fig. 4.

Table 3
Thermal properties of sand [36].

λ_L (m)	λ_T (m)	b_1 (W/m K)	b_2 (W/m K)	b_3 (W/m K)	C_s (MJ/m^3 K)	C_f (MJ/m^3 K)
0.05	0.01	0.228	−2.406	4.909	3.100	4.182

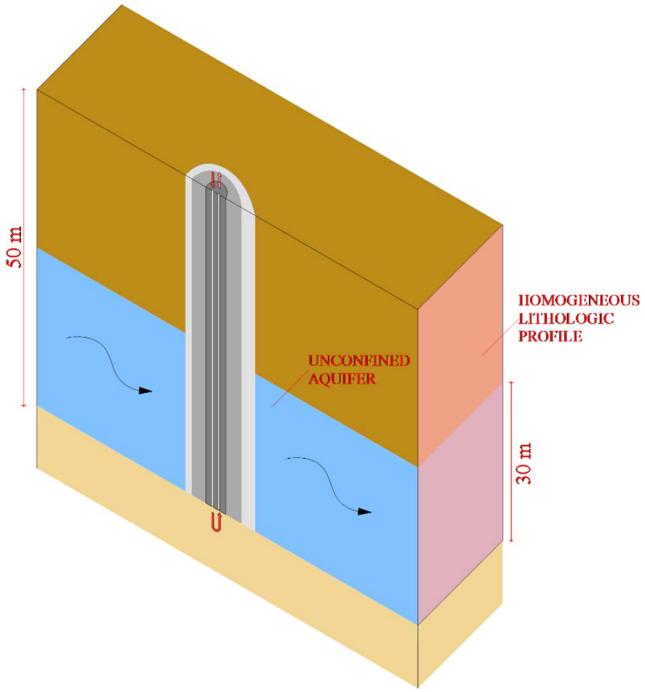

Fig. 4. A schematic of the modeling scenario used to investigate the influence of groundwater flow. The water flow is perpendicular to the borehole heat exchanger.

2.4.3. Layered soil profile

The assumption of a homogeneous and isotropic medium may not be valid for particular geological settings. Heterogeneities in subsurface thermal properties can significantly influence the heat transfer between the borehole heat exchanger and the surrounding soil [45]. However, in order to estimate thermal properties of each layer, it is necessary to include different types of measurements in the optimization process. When applying the conventional TRT, only the inlet and outlet fluid temperatures are usually available. In such circumstances, an inverse parameter estimation of thermal properties of multiple soil layers would cause parameter identification problems and increase the parameter uncertainty. If different types of measurements were available (e.g., fluid temperatures in the U-tube), it would be possible to better constrain the optimization problem, considering increased information content of experimental data. In such case, a proper modeling framework would include the use of a multi-objective optimization algorithm to obtain a trade-off between different likelihood functions assigned to each measurement. In this view, optical fibers represent a promising tool to retrieve important experimental data from borehole heat exchangers.

Optical fiber thermometers in geothermal wells started to be used in the late 1980s. Optical fibers can be used to measure the fluid temperature along the buried pipe of the exchanger. For example, Fujii et al. [46] conducted a series of TRTs using optical fibers in a U-tube borehole heat exchanger in Fukuoka, Japan. The measured fluid temperatures were then used to estimate the vertical distribution of thermal conductivities. In Fujii et al. [46], a cylindrical source function coupled with a nonlinear regression technique was applied. However, the fluid temperature was assumed to be constant during the circulation period, thus simplifying the problem. In another study, Acuña and Palm [47] proposed the use of optical fibers to measure the borehole wall temperature. The technique consisted of a fiber optic cable pressed against the borehole wall with a flexible plastic pipe that is filled with water once it is installed in the ground.

To demonstrate the capability of the newly-developed model to provide a comprehensive description of the heat transfer in a layered profile, a specific scenario has been simulated. In particular, a lithologic

Table 4
Simulated lithologic composition and soil distribution.

Depth (m)	*Soil type*
0–10	Loam
10–20	Sand
20–30	Clay
30–40	Sand
40–50	Clay

column composed of a series of sandy, clayey, and loamy soil layers has been considered. The exact soil distribution along the vertical depth is reported in Table 4.

A 50-m long U-tube borehole heat exchanger, similar to the one used at the TUAT experimental site, has been simulated. The pressure head was assumed to be -1 m and constant in the entire lithologic profile. Values reported in Chung and Horton [36] for loam, sand, and clay were used to characterize thermal properties. The input parameters (i.e., the U-tube thickness, fluid velocity, the inlet-outlet temperature difference, etc.) and other thermal properties were again the same as in the TUAT model validation. In order to highlight differences between homogeneous and heterogeneous systems, the results for the layered profile were compared with those for a homogeneous lithologic profile composed of sand.

For the sake of clarity, different modeling scenarios with their assumptions are summarized in Table 5.

3. Results and discussion

3.1. Model validation

Before proceeding with the model validation and further modeling scenarios, a mesh sensitivity analysis has been carried out. Results are summarized in Fig. 5, in which the outlet temperatures (Fig. 5, left) are reported for different values of N (the number of vertical elements) and corresponding computational costs (duration of simulations) (Fig. 5, right). Generally, finer discretizations are associated with more accurate numerical solutions since false numerical diffusion tends to vanish. At the first inspection, it is evident how the outlet temperature was relatively insensitive to the vertical mesh, underlining a general robustness of the proposed model. Simulated temperatures for $N = 5$ and $N = 10$ were almost the same (overlapped), indicating that a further mesh refinement would lead to negligible accuracy gains. Conversely, the results for $N = 2$ exhibited a slight overestimation of outflow temperatures, which can be related to the false numerical diffusion. However, the temperature difference at $t = 60{,}000$ s for $N = 2$ and $N = 5$ was only about 0.2 °C, which is still a relatively small error. On the other hand, the computational cost (Fig. 5, right) for $N = 2$ was only about half of that for $N = 10$, and also significantly lower than for $N = 5$. As a results of this analysis, a number of conclusions can be drawn:

– A coarse vertical mesh generally only introduces a low bias in the numerical solution, indicating that the model is relatively insensitive of the vertical mesh discretization;
– Considering the small numerical error and relatively low computational cost, the model with a coarse vertical mesh can be used when the aim of the analysis is to test different thermal properties of different materials (i.e., pipe, grout, and soil) and to simulate the outlet temperature;
– When the numerical analysis considers the effects of different layers, the groundwater table depth, and water flow on the thermal behavior of the borehole heat exchanger, a finer mesh should be used. In such cases, an additional preliminary mesh sensitivity analysis is required.
– Our analysis revealed that a value of $N = 5$ provided a good trade-off between computational cost and numerical accuracy. As a result, the model with $N = 5$ was used in the following modeling scenarios.

Table 5
Summary of modeling scenarios and their assumptions.

Scenario	Lithologic profile	Horizontal domain	Influence of water content
Model validation	Homogeneous	Circular	No
Morris sensitivity analysis	Homogeneous	Circular	No
Groundwater flow	Homogeneous	Squared	Yes
Groundwater depth	Homogeneous	Circular	Yes
Layered soil profile	Layered	Circular	Yes

The comparison between the measured and modeled outlet temperatures for both experimental sites is shown in Fig. 6. In particular, the simulated temperatures of the fluid at the outlet calculated using the values listed in Table 2 (red lines in Fig. 6) and the value of thermal conductivity obtained through the Line Source approach (Eq. (3)) (black lines in Fig. 6) are reported, respectively. The calculated *RMSEs* were 0.16 and 0.25 °C for the TUAT and SU experimental sites, respectively, when the best fit values were used. The low *RMSE* values confirmed the satisfactory accuracy of the proposed model in reproducing the behavior of the system. In both scenarios, the quality of the fit was sufficient, with a slightly better performance for the TUAT site. In particular, the model for the SU site slightly overestimated temperatures during the first 60,000 s of the simulation. This overestimation could be related to thermal properties of the grout material, whose influence is significant during the first part of the test. It must be emphasized that an improved fit could have been obtained by using an automatic optimization algorithm (e.g., Particle Swarm or Genetic Algorithm). However, this was not the aim of this study, which mainly focused on the development of a computationally efficient model. Future applications of the model can include the global optimization of thermal properties of different materials, as well as the sensitivity and uncertainty analysis.

The behavior was different when the values of thermal conductivity calculated using the Line Source approach (Eq. (3)) were used in the numerical simulations. In particular, the estimated *RMSEs* were 0.19 and 1.93 °C for the TUAT and SU experimental sites, respectively. In both cases, there was a degradation in terms of fitting quality, which was more evident for the SU site. For the TUAT, the model reproduced the thermal behavior of the BHE with sufficient accuracy. The assumption of homogeneous thermal properties led to a slight underestimation of the fluid temperature in the first part of the simulated period, which was mainly related to an overestimated value of the thermal conductivity of the grout. This bias tended to vanish for longer simulation periods. Conversely, the simulated thermal behavior of the borehole at the SU experimental site was quite different. In this case, the assumption of homogeneous thermal properties led to a significant overestimation of the fluid temperatures at the outlet, indicating a potential underestimation of the thermal conductivity of the grout. The deviation between the two models at $t = 120{,}000$ s is almost 2 °C. The analysis suggests an important role of the grout in the thermal behavior of the BHE. This aspect has been further investigated in the present study.

As shown in Fig. 7, the proposed model can calculate the temperature distribution in both the fluid and soil domains and at different time steps, providing an overall picture of the physics of the problem. At the beginning of the test ($t = 30{,}000$ s), it is evident that the heat transfer mainly affects the pipe and the grout, having only a limited influence on the surrounding soil. On the contrary, the soil is significantly heated after $t = 90{,}000$ s, especially near the surface where the effect of the heating system is important. The temperature

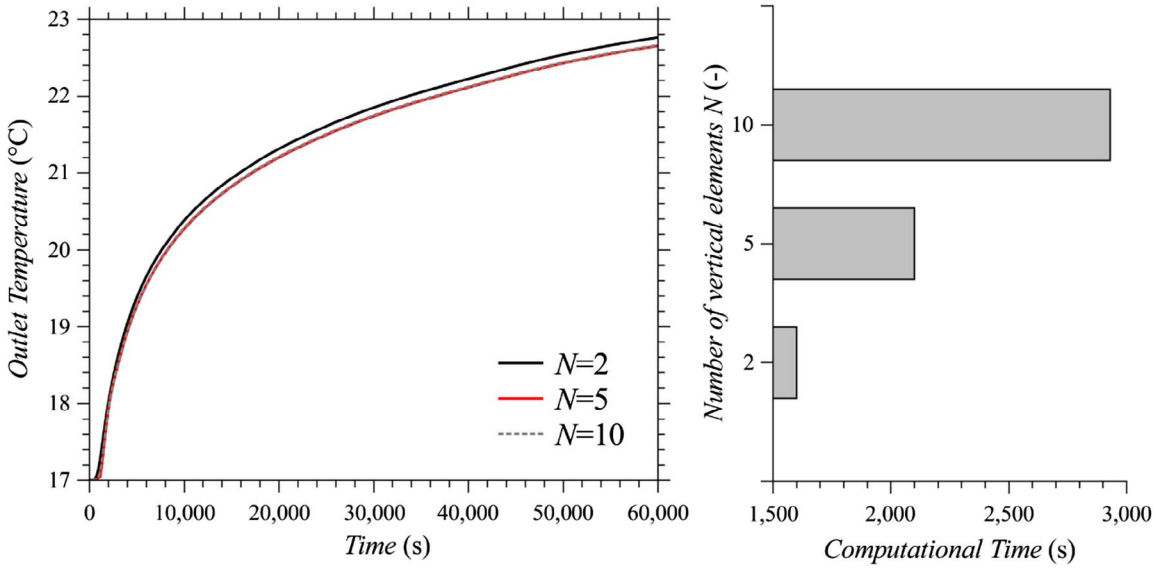

Fig. 5. Simulated outlet temperatures (left) for different values of N (the number of vertical elements) with their computational cost (right).

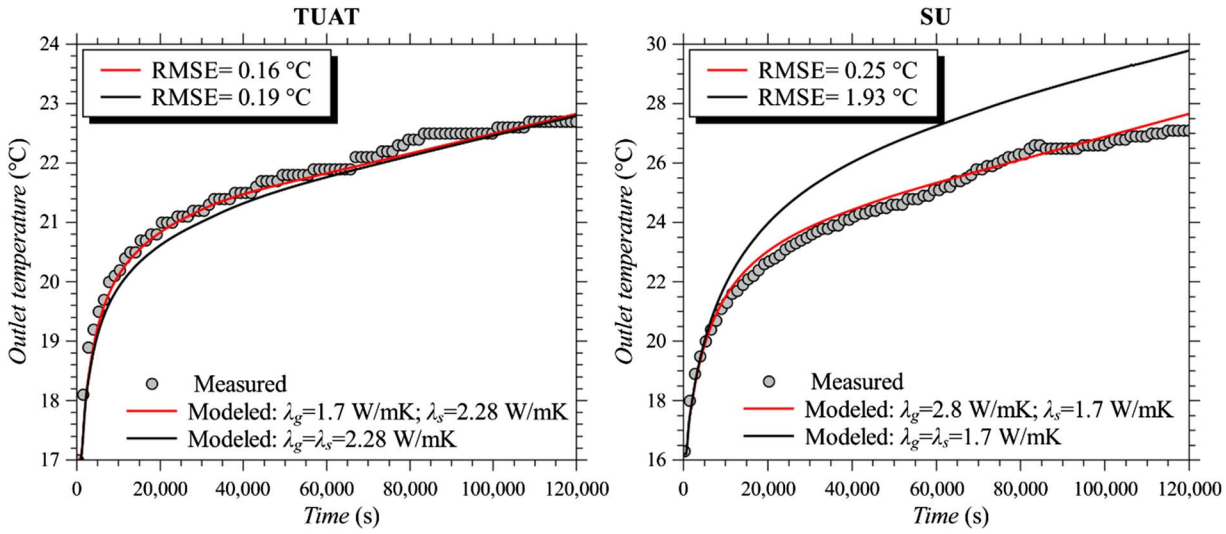

Fig. 6. Measured and modeled fluid temperatures at the tube/pipe outlet. Circles represent the measured fluid temperatures, black lines the modeled fluid temperatures calculated using the thermal conductivity obtained with the Kelvin line source equation, and red lines the modeled fluid temperatures calculated using the values reported in Table 2. (For interpretation of the references to color in this figure legend, the reader is referred to the web version of this article.)

distribution is asymmetric in the upper part of the domain, as it is expected for a U-tube borehole heat exchanger. It should be emphasized that the fluid temperature in both legs of the pipe appears smooth and devoid of nonlinearities. This behavior is directly related to the assumption of homogeneous soil. In this case, the convective heat transfer regulated by the Robin BC is not affected by inhomogeneities typical of layered lithologic profiles.

3.2. Sensitivity analysis

3.2.1. Morris method

The results of the sensitivity analysis, carried out using the Morris method, are reported in Fig. 8. In particular, the scatter plots μ^*–σ for two selected simulation times are shown.

At t = 10,800 s (left plot in Fig. 8), the thermal properties of the grout exhibited the highest μ^*, indicating a significant influence on the model's response. More specifically, the thermal conductivity of the grout λ_g was the most influential parameter, followed by the grout volumetric heat capacity C_g. The third most influential parameter was λ_p, which exhibited the highest σ value, indicating its important role in interactions with other factors. The volumetric heat capacity of the HDPE had a negligible effect on the model's response as highlighted by its low values of σ and μ^*, an expected behavior considering the limited diameter of the pipe. The thermal properties of the ground, λ_s and C_s, only had a limited influence on the output. Such behavior is intuitive, considering that in the first part of the test the ground is only partially involved in the heat transfer process, which is mainly driven by the grout and the pipe. This is emphasized in Fig. 8, in which two distinct groups can be identified: while parameters λ_g, C_g, and λ_p significantly influence the model's response, parameters λ_s, C_s, and C_p have only limited effects on the output.

The sensitivity measures significantly changed at t = 30,000 s (right plot in Fig. 8). As expected, the thermal properties of the soil increased their influence on the model's output, as indicated by their relatively high values of σ and μ^*. However, the grout and the pipe still had significant effects on the model's response. Contrary to what was highlighted at t = 10,800 s, it was very difficult to identify groups of parameters with distinct effects on the model behavior. The only

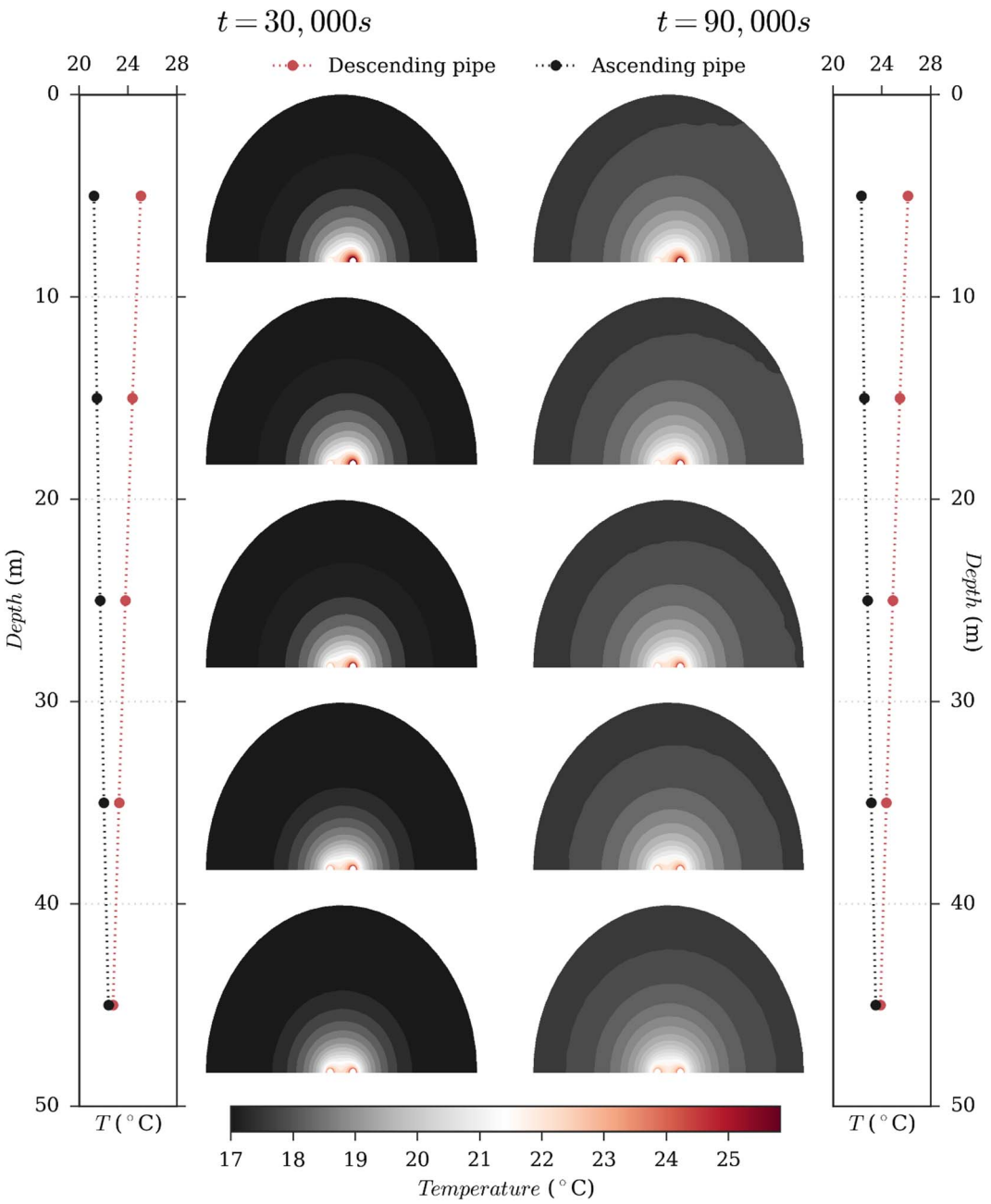

Fig. 7. The temperature distribution in both the fluid and horizontal two-dimensional domains at two different simulation times.

irrelevant factor was C_s, while the other parameters exhibited a relatively large impact.

The influence of λ_g and λ_s on the model's output has been further investigated in Fig. 9, which reports the outlet temperatures for different values of the grout (the left plot in Fig. 9) and ground (the right plot in Fig. 9) thermal conductivities. Blue arrows and dotted lines indicate increasing values of the thermal conductivity and the simulation times chosen for the Morris sensitivity analysis, respectively. The results were obtained by changing the value of the thermal conductivity while maintaining all other factors fixed. Fig. 8 confirmed the findings of the Morris sensitivity analysis. The influence of the grout was significant during the simulation, with a preeminent role in the first part of the experiment. This behavior is particularly evident when observing temperature values at two dotted lines. At t = 10,800 s, the model's output was mainly sensitive to λ_g, which generated a relatively high variance of temperatures. After 6000–8,000 s, the thermal conductivity of the ground started to have more important effects, which were more visible at t = 30,000 s.

The sensitivity analysis provided important information regarding the roles of different materials at different simulation times. In particular:

- The volumetric heat capacity of the pipe generally had a negligible effect on the model's output. In the optimization framework, this factor could be fixed to any feasible value in the parameter space without significantly affecting results.
- The thermal properties of the grout had a significant influence on the model's response during the first part of the simulation. This suggests that the thermal properties of the grout could be determined with reasonable accuracy by limiting the analysis to the first few hours of the simulation, in which the effect of the ground is rather limited. Considering only a short simulation period could speed up the numerical optimization, even if the model is computationally expensive. Moreover, the independent estimation of the

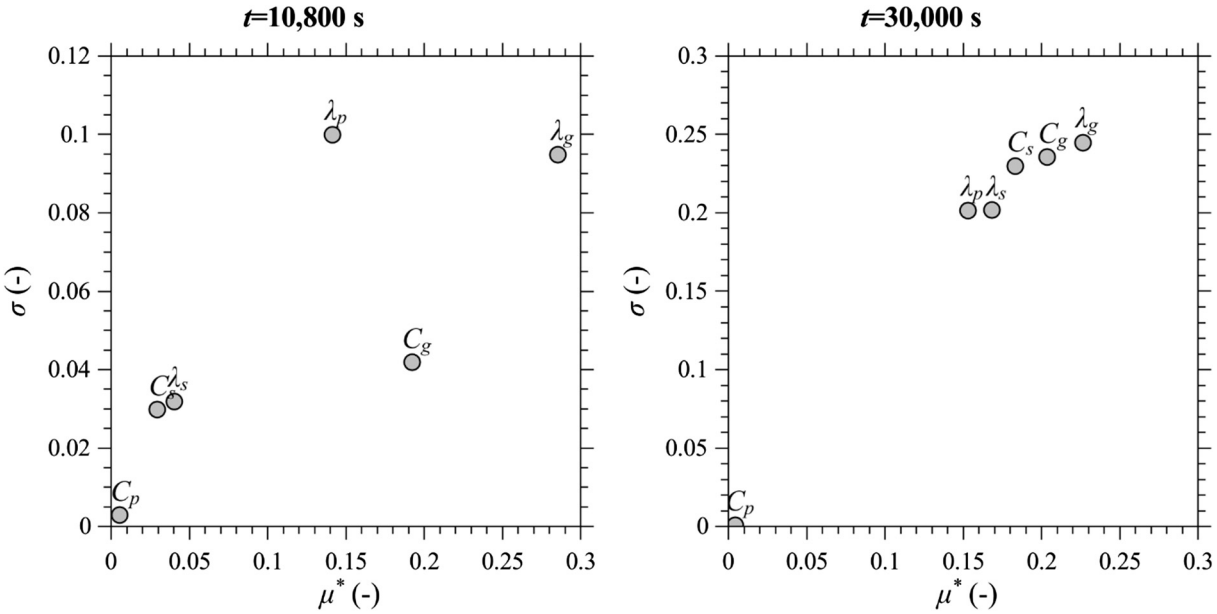

Fig. 8. Scatter plots of the Morris sensitivity measures for various thermal parameters (λ is the thermal conductivity, C is the thermal capacity, and subscripts p, g, and s refer to HDPE, grout, and soil, respectively) at two different simulation times (left t = 10,800 s and right t = 30,000 s).

thermal properties of the grout could significantly reduce the dimensionality of the subsequent optimization problem. This could be focused on the determination of the thermal properties of the ground, which is the core of the thermal response test.

– The effects of thermal properties of the ground on the model's output increased with time. It is important to temporally extend the numerical simulation to identify the thermal properties of the ground and limit the influence of the grout and the pipe. A short simulation time could lead to a biased estimation of the thermal properties.

3.2.2. Groundwater effects

The influence of groundwater on the TRT is shown in Fig. 10. In particular, the upper and lower figures show the effects of groundwater fluxes (0.0, $2.5 \cdot 10^{-6}$, and $5 \cdot 10^{-6}$ m/s) and aquifer thicknesses (10, 20, and 30 m), respectively. At the first inspection, it is evident that both aquifer thicknesses and groundwater fluxes are negatively correlated with the outlet temperatures of the fluid, indicating an increased heat dissipation in soil. This effect is more pronounced for increasing aquifer thicknesses, which indicates that large portions of the subsurface domain become saturated. In such circumstances, the soil becomes more conductive (Eq. (12)) and the heat transfer between the pipe and the soil is enhanced. Since saturation significantly affects thermal properties of soil, its effect becomes evident as soon as the soil is involved in the heat transfer process ($t \approx$ 10,000 s), similarly to what was indicated in the previous Morris sensitivity analysis. At t = 70,000 s, the largest deviation between simulated outlet temperatures is almost 1 °C and is kept almost constant for the remainder of the simulation.

This behavior is shown in detail in Fig. 11, in which temperature differences between the envelope curves (red and black lines in Fig. 10) are shown. The temperature difference increases significantly at the beginning of the simulation, indicating a significant influence of the aquifer thickness on the heat transfer process, and stabilizes around

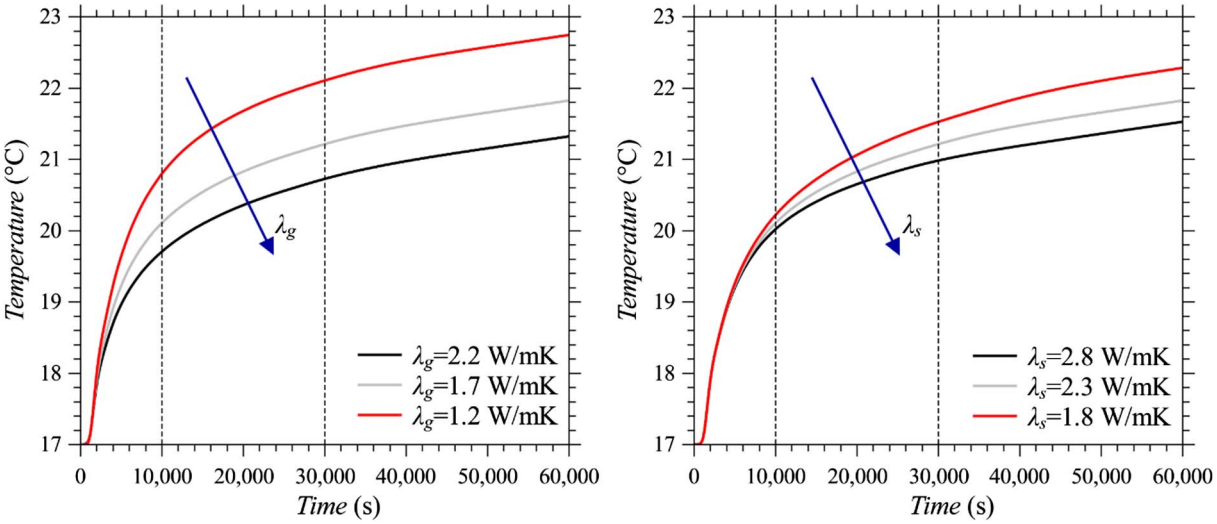

Fig. 9. The fluid temperature at the outlet for different values of the grout (left plot) and ground (right plot) thermal conductivities. Blue arrows indicate increasing values of the thermal conductivity. Dotted lines indicate the simulation times examined in the sensitivity analysis. (For interpretation of the references to color in this figure legend, the reader is referred to the web version of this article.)

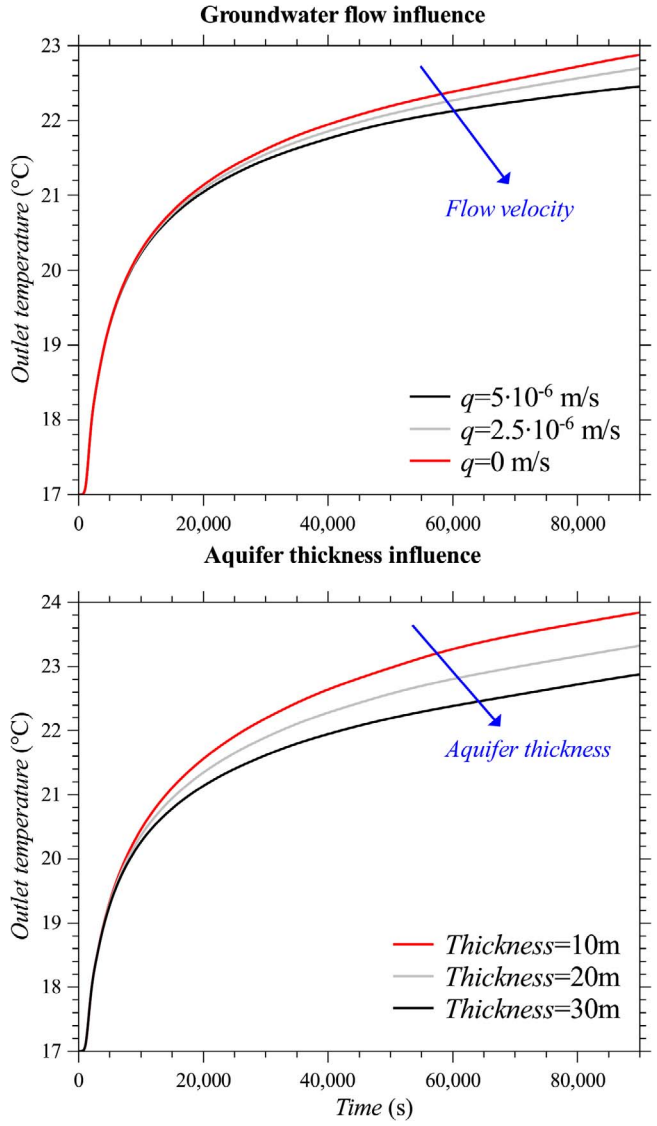

Fig. 10. Fluid temperatures at the outlet for different values of groundwater fluxes (the upper plot) and aquifer thicknesses (the lower plot). Blue arrows indicate increasing values of flux and thickness, respectively. (For interpretation of the references to color in this figure legend, the reader is referred to the web version of this article.)

t = 70,000 when it is almost 1 °C. This behavior is significantly different when examining the effect of groundwater flow. As shown in Fig. 10, the effect of groundwater flow becomes visually appreciable only after t = 20,000 s. The temperature difference increases almost linearly with time. At t = 40,000 s, its value is below 0.2 °C, indicating a limited influence on the system during the first part of the test. At t = 90,000 s, the temperature difference is about 0.4 °C. However, it must be emphasized that contrary to what was observed for the aquifer thickness, the temperature difference does not stabilize at this time, rather still exhibits an increasing trend. This indicates that the dissipation effect of groundwater flow is enhanced when the system becomes warmer.

The effect of different groundwater flow velocities on the heat transfer process is shown in Fig. 12, which displays three HYDRUS-2D cross sections for three different water fluxes. For q = 0 m/s, the distribution of temperatures is symmetric with a maximum value of 25.9 °C on the pipe surface. As the flux increases, the temperature field becomes asymmetric with a considerable amount of heat following saturated flow. The convective heat transport dissipates a significant amount of heat, thus lowering the temperature of the borehole heat

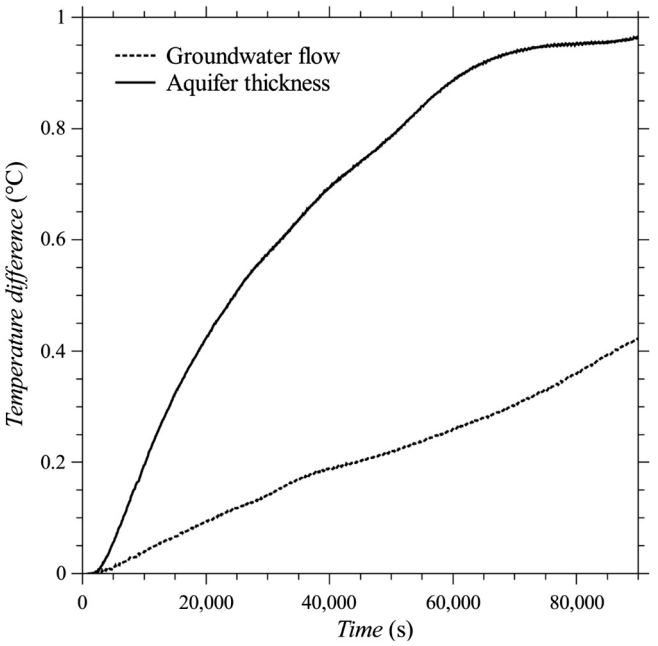

Fig. 11. Temperature differences between the two envelope curves (red and black lines in Fig. 6) for the aquifer thickness (solid line) and groundwater flow (dashed line). (For interpretation of the references to color in this figure legend, the reader is referred to the web version of this article.)

exchanger. It must be noted that the newly-developed model can provide a comprehensive description of the heat transfer in the entire system at a reduced computational cost compared to a fully 3D model.

3.2.3. Layered soil profile

The results of simulated scenario evaluating the effects of soil heterogeneity are presented in Fig. 13, which displays fluid temperatures in the U-tube for a homogeneous (lower plot in Fig. 13) and a layered (upper plot in Fig. 13) soil profile. At the first inspection, it is evident that the homogeneous profile, which is composed of sand, dissipates more heat compared to the layered scenario. The temperature difference is higher than 1 °C almost everywhere along the pipe. While the fluid temperature profile for the homogeneous soil is smooth, it exhibits some nonlinearities for the layered scenario. In particular, at the interface between clay and sand, the drift from the theoretical temperature profile for the homogeneous soil is significant. At a vertical depth of 15 m, the sandy layer causes a small increase in the concavity of the temperature curve, indicating an increase in the heat dissipation. On the contrary, at a vertical depth of 25 m, the temperature curve exhibits an inflection point due to the presence of the low-conductive clay layer, which in turn lowers the dissipation capacity of the surrounding soil.

It must be emphasized that, for the sake of simplicity and computational efficiency, only 5 Finite Volumes were used to discretize the lithologic profile. This example was meant to demonstrate the capabilities of the proposed modeling framework to handle layered profiles. Future applications can include the application of the model to real geological settings, with *ad hoc* mesh discretizations.

4. Conclusions and summary

The objective of the present study was to develop a computationally efficient pseudo-3D model for the analysis of Thermal Response Tests. The proposed modeling framework combines a one-dimensional description of the heat transport in the buried tubes of the exchanger with a two-dimensional description of the heat transfer in the surrounding subsurface soil, thus reducing the dimensionality of the problem and the computational cost. One of the main novelties of the study is the

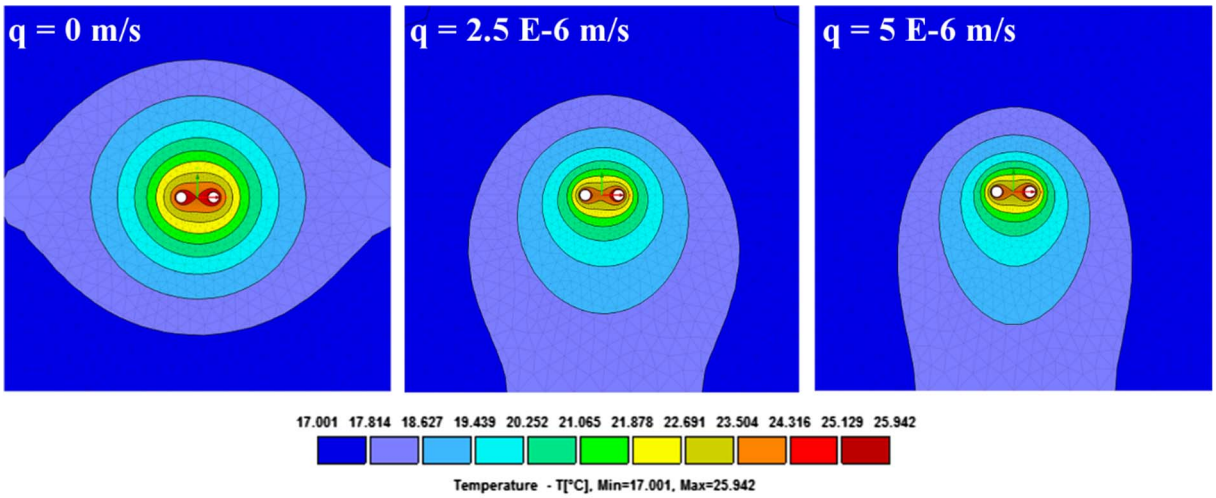

Fig. 12. HYDRUS-2D horizontal cross sections indicating the temperature distribution for three different values of groundwater flow at a depth of 45 m.

inclusion in the model of a widely used hydrological model, HYDRUS, which can describe the simultaneous movement of water, heat, and solutes in porous media. The proposed modeling approach is computationally efficient and the use of HYDRUS adds several important features that can be exploited not only in TRT but also in other engineering applications. The analysis demonstrated that the proposed model can reproduce the thermal behavior of borehole heat exchangers with good accuracy and that it can be exploited to investigate a variety of processes occurring in the vadose zone that affect the heat exchange (i.e., groundwater, flow, variably-saturated conditions, inhomogeneous lithologic profiles, etc.). Furthermore, the combination of the model with specific statistical techniques can clarify the influence of different factors on the thermal behavior of the borehole heat exchanger. In this view, the application of the Morris method represents a step forward compared to the traditional One-factor-at-a-time (OAT) techniques typically applied in this field since it guarantees a global exploration of the parameter space. Future work should investigate the use of different types of measurements for a more accurate determination of the thermal properties of the ground. Multi-objective optimization algorithms and Monte Carlo uncertainty procedures represent valuable tools for the inverse estimation of soil thermal properties, also in conjunction with surrogate models, which have proven to be rather useful in other engineering applications (e.g., Brunetti et al. [48]). Furthermore, a computational benchmark between existing models for borehole heat exchangers is suggested in order to compare the efficiency of different modeling frameworks.

Acknowledgements

The experimental part of this research was supported by Core Research for Evolutionary Science and Technology (CREST) from Japan Science and Technology Agency (JST). All TRT data analyzed in this study were collected with technical support from Mr. Eiji Yamashita of Agricluster Co Ltd, Japan.

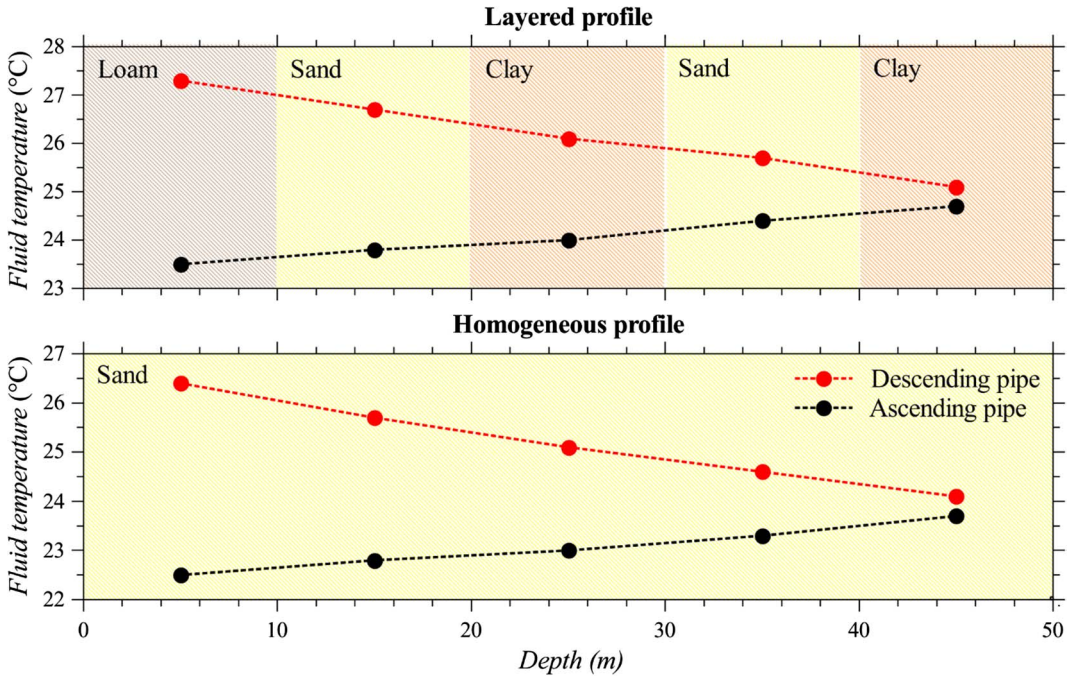

Fig. 13. Temperature profiles of the fluid in the U-tube for the layered (the upper plot) and homogeneous (the lower plot) lithologic profiles. The red and black lines indicate the descending and ascending legs of the U-tube, respectively.

References

[1] Lund JW, Boyd TL. Direct utilization of geothermal energy 2015 worldwide review. Geothermics 2016;60:66–93.
[2] Luo J, Rohn J, Bayer M, Priess A, Xiang W. Analysis on performance of borehole heat exchanger in a layered subsurface. Appl Energy 2014;123:55–65.
[3] Gehlin S. Thermal Response Test. Lulea University of Technology; 2002.
[4] Spitler JD, Gehlin SEA. Thermal response testing for ground source heat pump systems—an historical review. Renew Sustain Energy Rev 2015;50:1125–37.
[5] Carslaw HS, Jaeger JC. Conduction of heat in solids. 2nd ed. Oxford Clarendon Press; 1959.
[6] Ingersoll LR, Adler FT, Plass HJ, Ingersoll AC. Heat conduction with engineering, geological, and other applications. New York: McGraw-Hill; 1954.
[7] Wagner R, Clauser C. Evaluating thermal response tests using parameter estimation for thermal conductivity and thermal capacity. J Geophys Eng 2005;2:349–56.
[8] Bandos TV, Montero Á, Fernández de Córdoba P, Urchueguía JF. Improving parameter estimates obtained from thermal response tests: effect of ambient air temperature variations. Geothermics 2011;40:136–43.
[9] Hu P, Meng Q, Sun Q, Zhu N, Guan C. A method and case study of thermal response test with unstable heat rate. Energy Build 2012;48:199–205.
[10] Liuzzo-Scorpo A, Nordell B, Gehlin S. Influence of regional groundwater flow on ground temperature around heat extraction boreholes. Geothermics 2015;56:119–27.
[11] Wang H, Qi C, Du H, Gu J. Thermal performance of borehole heat exchanger under groundwater flow: a case study from Baoding. Energy Build 2009;41:1368–73.
[12] Hu J. An improved analytical model for vertical borehole ground heat exchanger with multiple-layer substrates and groundwater flow. Appl Energy 2017;202:537–49.
[13] Liuzzo Scorpo A, Nordell B, Gehlin S. A method to estimate the hydraulic conductivity of the ground by TRT analysis. Groundwater 2017;55:110–8.
[14] Rainieri S, Bozzoli F, Pagliarini G. Modeling approaches applied to the thermal response test: a critical review of the literature. HVAC & R Res 2011;17:977–90.
[15] Shonder JA, Beck JV. A new method to determine the thermal properties of soil formations from in situ field tests; 2000.
[16] Florides GA, Christodoulides P, Pouloupatis P. Single and double U-tube ground heat exchangers in multiple-layer substrates. Appl Energy 2013;102:364–73.
[17] Ozudogru TY, Olgun CG, Senol A. 3D numerical modeling of vertical geothermal heat exchangers. Geothermics 2014;51:312–24.
[18] Han C, Yu X. (Bill). Sensitivity analysis of a vertical geothermal heat pump system. Appl Energy 2016;170:148–60.
[19] Signorelli S, Bassetti S, Pahud D, Kohl T. Numerical evaluation of thermal response tests. Geothermics 2007;36:141–66.
[20] Kohl T, Hopkirk RJ. "FRACTure" – a simulation code for forced fluid flow and transport in fractured, porous rock. Geothermics 1995;24:333–43.
[21] Bozzoli F, Pagliarini G, Rainieri S, Schiavi L. Estimation of soil and grout thermal properties through a TSPEP (two-step parameter estimation procedure) applied to TRT (thermal response test) data. Energy 2011;36:839–46.
[22] Christodoulides P, Florides GA, Pouloupatis P, Messaritis V, Lazari L. Ground heat exchanger modeling developed for energy flows of an incompressible fluid. Int J Mech Aerospace, Inductrial, Mechatron Manuf Eng 2012;6:640–4.
[23] Kim E-JJ, Roux J-JJ, Rusaouen G, Kuznik F. Numerical modelling of geothermal vertical heat exchangers for the short time analysis using the state model size reduction technique. Appl Therm Eng 2010;30:706–14.
[24] Šimůnek J, van Genuchten MT, Šejna M. Recent developments and applications of the HYDRUS computer software packages. Vadose Zo J 2016;15:25.
[25] Morris MD. Factorial sampling plans for preliminary computational experiments. Technometrics 1991;33:161–74.
[26] Thuyet DQ, Saito H, Saito T, Moritani S, Kohgo Y, Komatsu T. Multivariate analysis of trace elements in shallow groundwater in Fuchu in western Tokyo Metropolis. Japan. Environ Earth Sci 2016;75:559.
[27] Saito T, Hamamoto S, Ueki T, Ohkubo S, Moldrup P, Kawamoto K, et al. Temperature change affected groundwater quality in a confined marine aquifer during long-term heating and cooling. Water Res 2016;94:120–7.
[28] Saito T, Hamamoto S, Ei Mon E, Takemura T, Saito H, Komatsu T, et al. Thermal properties of boring core samples from the Kanto area, Japan: development of predictive models for thermal conductivity and diffusivity. Soils Found 2014;54:116–25.
[29] Yavuzturk C, Spitler JD, Simon PE, Rees J. A transient two-dimensional finite volume model for the simulation of vertical U-Tube ground heat exchangers. ASHRAE Trans 1999;105(2):465–74.
[30] Austin W, Yavuzturk C, Spitler JD. Development of an in-situ system for measuring ground thermal properties. ASHRAE Trans 2000;106(1):365–79.
[31] Gustafsson AM, Gehlin S. Influence of natural convection in water-filled boreholes for GCHP. ASHRAE Trans 2008;114(PART 1):416–23.
[32] Spitler JD, Javed S, Ramstad RK. Natural convection in groundwater-filled boreholes used as ground heat exchangers. Appl Energy 2016;164:352–65.
[33] Choi W, Ooka R. Effect of natural convection on thermal response test conducted in saturated porous formation: comparison of gravel-backfilled and cement-grouted borehole heat exchangers. Renew Energy 2016;96:891–903.
[34] Hellström G, Tsang C-F, Claesson J. Buoyancy flow at a two-fluid interface in a porous medium: analytical studies. Water Resour Res 1988;24:493–506.
[35] Leonard BP. A stable and accurate convective modelling procedure based on quadratic upstream interpolation. Comput Methods Appl Mech Eng 1979;19:59–98.
[36] Chung S-O, Horton R. Soil heat and water flow with a partial surface mulch. Water Resour Res 1987;23:2175–86.
[37] Beier RA, Smith MD, Spitler JD. Reference data sets for vertical borehole ground heat exchanger models and thermal response test analysis. Geothermics 2011;40:79–85.
[38] Zhang C, Guo Z, Liu Y, Cong X, Peng D. A review on thermal response test of ground-coupled heat pump systems. Renew Sustain Energy Rev 2014;40:851–67.
[39] Saito H, Saito T, Kohgo Y, Hamamoto S, Moldrup P, Komatsu T. Effect of reducing the test period on estimating effective thermal conductivity from Kelvin's line source function in thermal response test: a numerical study. J Jpn Soc Soil Phys 2014;128:11–20.
[40] Florides GA, Christodoulides P, Pouloupatis P. An analysis of heat flow through a borehole heat exchanger validated model. Appl Energy 2012;92:523–33.
[41] Wagner V, Bayer P, Kübert M, Blum P. Numerical sensitivity study of thermal response tests. Renew Energy 2012;41:245–53.
[42] Campolongo F, Cariboni J, Saltelli A. An effective screening design for sensitivity analysis of large models. Environ Model Softw 2007;22:1509–18.
[43] Gehlin SEA, Hellström G. Influence on thermal response test by groundwater flow in vertical fractures in hard rock. Renew Energy 2003;28:2221–38.
[44] Raymond J, Therrien R, Gosselin L, Lefebvre R. Numerical analysis of thermal response tests with a groundwater flow and heat transfer model. Renew Energy 2011;36:315–24.
[45] Fujii H, Okubo H, Nishi K, Itoi R, Ohyama K, Shibata K. An improved thermal response test for U-tube ground heat exchanger based on optical fiber thermometers. Geothermics 2009;38:399–406.
[46] Fujii H, Okubo H, Itoi R. Thermal response tests using optical fiber thermometers. Geotherm Resour Counc Trans 2006;30:545–51.
[47] Acuña J, Palm B. Distributed thermal response tests on pipe-in-pipe borehole heat exchangers. Appl Energy 2013;109:312–20.
[48] Brunetti G, Šimůnek J, Turco M, Piro P. On the use of surrogate-based modeling for the numerical analysis of low impact development techniques. J Hydrol 2017;548:263–77.